



Universiteit  
Leiden  
The Netherlands

**Mechanism-based pharmacokinetic-pharmacodynamic modelling of opioids : role of biophase distribution and target interaction kinetics**  
Groenendaal, D.

**Citation**

Groenendaal, D. (2007, September 18). *Mechanism-based pharmacokinetic-pharmacodynamic modelling of opioids : role of biophase distribution and target interaction kinetics*. Retrieved from <https://hdl.handle.net/1887/12321>

Version: Corrected Publisher's Version

License: [Licence agreement concerning inclusion of doctoral thesis in the Institutional Repository of the University of Leiden](#)

Downloaded from: <https://hdl.handle.net/1887/12321>

**Note:** To cite this publication please use the final published version (if applicable).

**Section 3**  
**PHARMACOKINETIC-PHARMACODYNAMIC**  
**MODELLING OF THE EEG EFFECTS OF OPIOIDS**

Sec3



Chapter 7  
**PHARMACOKINETIC-PHARMACODYNAMIC  
MODELLING OF THE EEG EFFECTS OF OPIOIDS:  
THE ROLE OF COMPLEX BIOPHASE DISTRIBUTION  
KINETICS**

Dorien Groenendaal<sup>1</sup>, Jan Freijer<sup>2</sup>, Andrea Rosier<sup>1</sup>, Dennis de Mik<sup>1</sup>, Glynis Nicholls<sup>3</sup>,  
Anne Hersey<sup>4</sup>, Andrew D Ayrton<sup>3</sup>, Meindert Danhof<sup>1,2</sup> and Elizabeth C.M. de Lange<sup>1</sup>

<sup>1</sup>Leiden/Amsterdam Center for Drug Research, Leiden University, Division of Pharmacology,  
Leiden, The Netherlands, <sup>2</sup>LAP&P Consultants BV, Leiden, The Netherlands, <sup>3</sup>GlaxoSmithKline,  
Drug Metabolism and Pharmacokinetics, Ware, United Kingdom, <sup>4</sup>GlaxoSmithKline,  
Computational and Structural Sciences, Stevenage, United Kingdom

*Submitted for publication*

## ABSTRACT

The objective of this investigation was to characterize the role of complex biophase distribution kinetics in the pharmacokinetic-pharmacodynamic correlation of a wide range of opioids. Following intravenous infusion of morphine, alfentanil, fentanyl, sufentanil, butorphanol and nalbuphine the time course of the EEG effect was determined in conjunction with blood concentrations. Different biophase distribution models were tested for their ability to describe hysteresis between blood concentration and effect. For morphine, hysteresis was best described by an extended catenary biophase distribution model with different values for  $k_{1e}$  and  $k_{e0}$  of  $0.038 \pm 0.003$  and  $0.043 \pm 0.003 \text{ min}^{-1}$ , respectively. For the other opioids hysteresis was best described by a one-compartment biophase distribution model with identical values for  $k_{1e}$  and  $k_{e0}$ . Between the different opioids, the values of  $k_{1e}$  ranged from 0.04 and  $0.47 \text{ min}^{-1}$ . The correlation between concentration and EEG effect was successfully described by the sigmoidal Emax pharmacodynamic model. Between opioids significant differences in potency ( $EC_{50}$  range: 1.2 - 451 ng/ml) and intrinsic activity ( $\alpha$  range: 18 -109  $\mu\text{V}$ ) were observed.

In addition, membrane transport characteristics of the opioids were investigated *in vitro*, using MDCK:MDR1 cells and *in silico* with QSAR analysis. A statistically significant correlation was observed between the values of the *in vivo*  $k_{1e}$  and the apparent passive permeability as determined *in vitro* in MDCK:MDR1 monolayers.

It is concluded that unlike other opioids, only morphine displays complex biophase distribution kinetics, which can be explained by its relatively low passive permeability and the interaction with active transporters at the blood-brain barrier.

## INTRODUCTION

Biophase distribution kinetics can be an important determinant of the pharmacokinetic-pharmacodynamic (PK-PD) correlations of CNS active drugs, and is often described by a one-compartment biophase distribution model, also known as the effect-compartment model. With the effect compartment model the assumption is made that the rate of onset and offset of the drug effect is governed by the rate of drug distribution to the hypothetical "effect-site" (Sheiner *et al.* 1979). This effect-compartment is then linked to the blood concentrations with the rate constant  $k_{1e}$  and the rate constant for drug loss  $k_{e0}$ . Typically, the biophase distribution is considered to be symmetrical under the assumption that in equilibrium the effect-site concentration equals the blood concentration, in other words, where  $k_{1e}$  is equal to  $k_{e0}$ . However, also more complex biophase distribution models have been proposed. For example, for the neuroactive steroid alphaxolone a concentration dependent  $k_{e0}$  was observed (Visser *et al.* 2002). It was shown that the  $k_{e0}$  was correlated to the  $C_{max}$  in plasma. In addition, Mandema and co-workers have reported two equilibration rate constants for the dual effects of heptabarbital and have shown that the equilibration kinetics of amobarbital were best described with a bi-exponential transducer function instead of a simple first-order mono-exponential equilibration model (Mandema & Danhof 1990; Mandema *et al.* 1991b).

For opioids, modelling of complex biophase distribution kinetics is of interest, given the interaction with active transporters and the wide range in lipophilicity. In previous investigations, morphine and loperamide have been identified as substrates for P-glycoprotein (Pgp) in both *in vitro* and *in vivo* models (Letrent *et al.* 1999b; Mahar Doan *et al.* 2002; Schinkel *et al.* 1995; 1996; Wandel *et al.* 2002). Furthermore, PK-PD studies in rats have revealed that after oral pre-treatment with the specific Pgp inhibitor GF120918, the anti-nociceptive effect of morphine was prolonged due to its prolonged half-life in the brain (Letrent *et al.* 1998; 1999a). Alfentanil and sufentanil were not identified as Pgp substrates within the abovementioned *in vitro* studies, whereas inconsistencies have been reported for fentanyl (Henthorn *et al.* 1999; Wandel *et al.* 2002). In addition, for fentanyl, *in situ* brain perfusion studies indicated Pgp mediated efflux (Dagenais, Graff, & Pollack 2004). Nalbuphine, a semi-synthetic opioid analgesic, was also found to be a Pgp substrate in a MDCKII-MDR1 cell-system (Mahar Doan *et al.* 2002), whereas to our knowledge so far no studies have been performed on butorphanol.

In order to study the differences in biophase distribution kinetics between opioids, an *in vivo* model is required that is able to study changes in pharmacological effects in great detail. Previous investigations have shown that quantitative analysis of the increase in the delta frequency band of the electroencephalogram (EEG) is a suitable biomarker for the PK-PD correlation of opioids (Cox *et al.* 1998; Groenendaal *et al.* 2007 - chapter 6).

PK-PD analysis with the one-compartment biophase distribution model showed that only small differences were observed between alfentanil, fentanyl and sufentanil, no hysteresis ( $k_{eo}$ ) was observed for alfentanil, whereas for fentanyl and sufentanil the  $k_{eo}$  values were  $0.32 \text{ min}^{-1}$  and  $0.17 \text{ min}^{-1}$ , respectively. In this analysis, all opioids behaved as full agonists with an intrinsic activity of around  $100 \mu\text{V}$ , but differed in potency ( $\text{EC}_{50}$  values of  $1.43 - 289 \text{ ng/ml}$ ). For morphine profound hysteresis was observed between the blood pharmacokinetics and EEG effects. Co-infusion of the Pgp inhibitor GF120918 prolonged the offset of the EEG effect but had no influence on the onset of the hysteresis. The biophase distribution kinetics were best described with the extended-catenary biophase distribution model, consisting of two sequential effect compartments (i.e. a transfer and an effect compartment) and two rate constants for transport through the transfer compartment ( $k_{1e}$ ) and for loss from the effect compartment ( $k_{e0}$ ) (Groenendaal *et al.* 2007 – chapter 6). In this study, morphine behaved as a low efficacy agonist with an intrinsic activity of  $44.5 \mu\text{V}$ .

The objective of the study presented here was to study the biophase distribution kinetics in the PK-PD correlation of a wide range of opioids. The opioids selected were alfentanil, fentanyl, sufentanil, morphine, butorphanol and nalbuphine (figure 1).

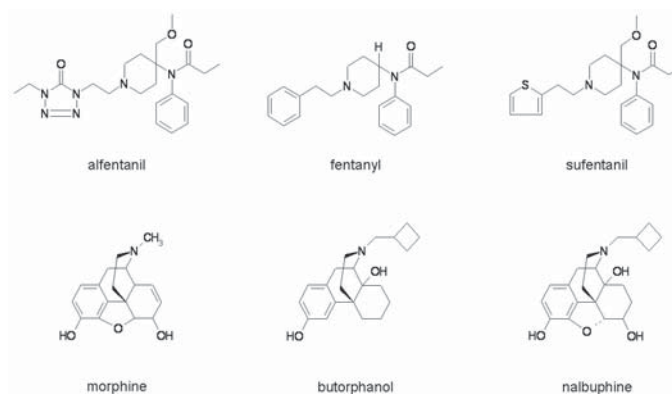


**Figure 1:** Chemical structures of the opioids. The individual names of the compounds are depicted below the chemical structures.

Nalbuphine and butorphanol were added because they behave as partial agonists *in vivo* (Emmerson *et al.* 1996). The biophase distribution kinetics was investigated with both the one-compartment biophase distribution model, and the extended-catenary biophase distribution model as previously proposed for morphine (Groenendaal *et al.*, 2007 – chapter 6). *In vitro* and *in silico* studies were also included to investigate the membrane transport characteristics of all the opioids with respect to P-glycoprotein interaction, apparent membrane permeability and physico-chemical properties. The predicted effect-site concentrations were related to the EEG effect on basis of the sigmoidal  $E_{\text{max}}$  pharmacodynamic model.

## MATERIALS AND METHODS

### *Animals and surgical procedures*

The protocol of these studies was approved by the Committee of Animal Experimentation of the Leiden University. Male Wistar rats weighing between 250-350 grams were housed in groups for at least 7 days under standard environmental conditions (temperature 21 °C, humidity 60% and 12/12 hour dark/light cycle, with lights on at 7 a.m.). The animals had access to standard laboratory chow (RMH-TM, Hope Farms, Woerden, The Netherlands) and acidified water *ad libitum*.

Nine days before the start of the experiments, seven cortical electrodes were implanted into the skull as described before (Cox *et al.* 1997). Briefly, the electrodes were placed at the locations 11 mm anterior and 2,5 mm lateral ( $F_1$  and  $F_r$ ), 3 mm anterior and 3,5 mm lateral ( $C_1$  and  $C_r$ ) and 3 mm posterior and 2,5 mm lateral ( $O_1$  and  $O_r$ ) to lambda. A reference electrode was placed on lambda. Stainless-steel screws were used as electrodes and connected to a miniature connector, which was insulated and fixed to the skull with dental acrylic cement.

Two days before the start of the experiments, three/four indwelling cannulas were implanted, one in the right femoral artery for collection of serial blood samples and two in the left jugular vein (interna and externa) for opioid and midazolam administration. The fourth cannula was implanted into the right femoral vein to administer vecuronium bromide which was only required for the experiments with alfentanil, fentanyl, sufentanil and morphine. All cannulas were made from pyrogen free polyethylene tubing (Portex Limited, Hythe, Kent, United Kingdom). The arterial cannula consisted of 4 cm (I.D.=0.28, O.D.=0.61 mm) polyethylene tubing heat-sealed to 18 cm polyethylene tubing (I.D.=0.58, O.D.=0.96 mm). The venous cannula consisted of 3 cm (I.D.=0.28, O.D.=0.61 mm) polyethylene tubing heat-sealed to 10 cm polyethylene tubing (I.D.=0.58, O.D.=0.96 mm). The cannulas were subcutaneously tunnelled to the back of the neck of the rats. In order to prevent clotting the cannulas were filled with a 25% (w/v) polyvinylpyrrolidone (PVP, Brocacef, Maarssen, The Netherlands) solution in saline containing 50 IU/ml heparin (Pharmacy, Leiden University Medical Centre, Leiden, The Netherlands).

All rats were anesthetized with an intramuscular injection of 0.1 mg/kg Domitor® (1 mg/ml medetomidine hydrochloride, Pfizer, Capelle a/d IJssel, The Netherlands) and subcutaneous injection of 1 mg/kg Ketalar® (50 mg/ml Ketaminebase, Parke-Davis, Hoofddorp, The Netherlands). After the first surgery, 4 mg ampicilline (A.U.V., Cuijk, The Netherlands) was administered to aid recovery.

### *Drugs and dosages*

Alfentanil hydrochloride, fentanyl citrate and sufentanil citrate were kindly donated by Johnson& Johnson Pharmaceutical Research and Development, a Division of Janssen



Pharmaceutica N.V (Beerse, Belgium). Morphine hydrochloride was purchased from Pharmachemie (Haarlem, The Netherlands), nalbuphine hydrochloride and nalorphine hydrochloride were purchased from Sigma Aldrich (Zwijndrecht, The Netherlands) and butorphanol tartrate was purchased from Sigma Aldrich (St. Louis, MI, USA). Midazolam was obtained from BUFA (Uitgeest, The Netherlands). Vecuronium bromide (Norcuron<sup>®</sup>) was obtained from the hospital pharmacy of the Leiden University Medical Center (Leiden, The Netherlands).

Solutions of the opioids were prepared in physiological saline (0.9%) on the day of the experiment. 500-1500  $\mu$ l of the infusion solution was administered to each rat. The doses and concentrations are expressed as free base and the concentrations of the infusion solutions were based on the body weight of each rat. Midazolam was administered to prevent opioid induced seizures at a rate of 5.5 mg/kg/h (Cox *et al.* 1997). To reach steady state rapidly, midazolam was administered according to a Wagner infusion scheme, with an initial infusion rate of 3 times the steady state infusion rate for 16 min (Wagner 1974). Vecuronium bromide solutions were prepared at a concentration of 2 mg/ml in physiological saline, independent of body weight.

#### *Pharmacokinetic/pharmacodynamic experiments*

The original data and details of the experiments with alfentanil, fentanyl, sufentanil and morphine have been published previously (Cox *et al.* 1998; Groenendaal *et al.* 2007 – chapter 6). The experimental protocols for nalbuphine and butorphanol were similar as described for alfentanil, fentanyl and sufentanil. Animals were randomly assigned to the treatment groups. Detailed information regarding the complete experimental design are shown in table 1.

All experiments were started between 8.30 and 9.30 a.m. to minimize influences of circadian rhythms. During the experiments, the animals were deprived of food and water. Bipolar EEG leads on the left hemisphere ( $C_1-O_1$ ) were continuously monitored using a Nihon-Kohden AB-621G Bioelectric Amplifier (Hoekloos BV, Amsterdam, The Netherlands) and concurrently digitized at a rate of 256 Hz using a CED 1401plus interface (CED, Cambridge, United Kingdom). The digitized signal was transferred into a Pentium III computer and stored on hard disk for off-line analysis. For each 5-sec epoch, quantitative EEG parameters were obtained off-line by Fast Fourier Transformation with a user-defined script within the software package Spike2 for Windows, version 3.18 (CED, Cambridge, United Kingdom). Changes in the amplitudes in the  $\delta$ -frequency band of the EEG (0.5-4.5 Hz) averaged over 1-minute time intervals were used as a pharmacodynamic endpoint. Further reduction of the EEG data was performed by averaging the signals over predetermined time intervals using a user-defined script within the software package Matlab<sup>®</sup>, version 6.1 (The Mathworks Inc., Gouda, The Netherlands).

**Table 1:** Experimental design of the studies investigating the PK-PD relationships of the EEG effects of opioids.

Compound	N	Dose (mg/kg)	Infusion time (min)	Body weight (kg)
Morphine <sup>b</sup>	24	4	10	0.297 ± 0.003
	7	10	10	0.260 ± 0.006
	18	40	10	0.298 ± 0.006
Alfentanil <sup>a</sup>	7	3.14	40	0.278 ± 0.005
Fentanyl <sup>a</sup>	8	0.15	20	0.290 ± 0.012
Sufentanil <sup>a</sup>	7	0.03	40	0.297 ± 0.006
Butorphanol	7	2.5	10	0.284 ± 0.006
	6	5	10	0.260 ± 0.002
	6	10	10	0.254 ± 0.004
Nalbuphine	6	5	10	0.275 ± 0.009
	9	10	10	0.273 ± 0.006
	5	15	10	0.283 ± 0.006 <sup>c</sup>
Saline	6	n/a	10	0.290 ± 0.007

<sup>a</sup>Experiments described previously by Cox et al. 1997

<sup>b</sup>Experiments described previously by Groenendaal et al. 2006

<sup>c</sup>Not included in the analysis because of severe systemic side effects during and after the opioid infusion

The EEG baseline was recorded for 15 min. Thereafter, midazolam infusion was started. 30 minutes after the start of the midazolam infusion, the opioids were administered in a zero-order infusion using a BAS Beehive infusion pump (Bioanalytical systems Inc., Indiana, USA). The EEG signals were recorded up to a maximum of 360 minutes after start of the opioid infusions. For determination of opioid and midazolam concentrations, serial arterial blood samples were collected at predetermined time intervals and immediately hemolysed with 0.5 ml of millipore water and stored at -20 °C.

During and after the infusion of the opioids, respiratory depression occurred. Arterial blood samples were collected to monitor arterial pH, pO<sub>2</sub> and pCO<sub>2</sub> levels using a Corning 248 Blood Gas Analyzer (Bayer, Mijdrecht, The Netherlands). During and after administration of 40 mg/kg morphine, alfentanil, fentanyl and sufentanil, severe respiratory depression and muscle rigidity occurred. These rats were artificially ventilated with preheated air (32 °C) using an Amsterdam Infant Ventilator, model MK3 (Hoekloos, Amsterdam, The Netherlands) through a custom made ventilation mask as described by Cox and co-workers (1997). The ventilation settings were: ventilation frequency 62 beats/min, I-E ratio 1:2 and air supply flow rate 0.7-1.0 l/min. 5 minutes after start of the infusion, the rats received an intravenous bolus dose of 0.15 mg vecuronium bromide and artificial ventilation was started. Vecuronium doses of 0.10 mg were administered repeatedly when muscle rigidity re-appeared until respiratory activity resumed. Blood gas status was carefully monitored during the whole experiment.

During the experiments, body temperature was stabilized between 37.5 and 38.5 °C using a CMA/140 temperature controller (Aurora Borealis, Schoonebeek, The Netherlands).

### *Drug analysis*

The analysis methods for the opioids in blood samples have been described previously (Cox *et al.* 1997; 1998; Groenendaal *et al.* 2005 – chapter 3). The blood concentrations of alfentanil were determined by gas chromatography with nitrogen-phosphorus detection, after a liquid-liquid extraction of the hemolyzed blood samples with sodium triphosphate and pentane. The intra- and interassay variability was generally less than 5% and the lower limit of quantification was 1 ng/ml for a 0.1 ml sample. The blood concentrations of fentanyl and sufentanil were determined by radio-immunoassay, after liquid-liquid extraction of the samples with sodium hydroxide and n-heptane/isoamylalcohol (98.5/1.5, v/v). The intra- and inter-assay variability were less than 40% and the lower limits of quantification were 0.040 ng/ml for a 1 ml sample obtained at the end of the experiment for both fentanyl and sufentanil.

Morphine, nalbuphine and butorphanol blood samples were analyzed by an HPLC method coupled to an electrochemical detector, after a liquid-liquid extraction of the hemolyzed blood samples with phosphoric acid and/or sodium carbonate and ethyl acetate. The intra- and inter-assay variation was less than 15% for morphine, nalbuphine and butorphanol. The lower limits of quantification for a 50 µl blood sample were 25, 25 and 50 ng/ml for morphine, nalbuphine and butorphanol, respectively (Groenendaal *et al.* 2005 – chapter 3).

The blood concentrations of midazolam were determined as described previously by Mandema and co-workers (Mandema *et al.* 1991a). The method consisted of a liquid-liquid extraction with NaOH and dichloromethane/petroleum ether (45/55, v/v). After extraction, samples were injected onto an HPLC coupled to an ultraviolet detector. The intra- and inter-assay variation was less than 6% and the lower limit of quantification was 50 ng/ml for a 50 µl blood sample.

### *Pharmacokinetic-pharmacodynamic data analysis*

The pharmacokinetic and pharmacodynamic data of the opioids were analysed using non-linear mixed effect modelling as implemented in the NONMEM software version V, level 1.1 (Beal & Sheiner 1999). Population analysis was undertaken using the first-order conditional estimation method (FOCE interaction) for pharmacokinetic analysis. All fitting procedures were performed on an IBM-compatible computer (Pentium IV, 1500 MHz) running under Windows XP with the Fortran Compiler Compaq Visual Fortran version 6.1.

### *Pharmacokinetic analysis*

For the development of the pharmacokinetic structural models for the opioids, both two- and three-compartment models were tested. Model selection was based on the likelihood ratio test, diagnostic plots (observed concentrations vs. individual and population predicted concentrations, weighted residuals vs. predicted time and concentrations), parameter correlations and precision in parameter estimates. The likelihood criteria

test is based on a comparison of the minimum value of the objective function (MVOF) of two models. The significance level was set at 0.01 which corresponds to a decrease of MVOF of 6.6 points when an extra parameter is included in the structural model under the assumption that the difference in MVOF between the two nested models is  $\chi^2$  distributed. On the basis of model selection criteria a three-compartment model was chosen for alfentanil, morphine and nalbuphine, whereas a two-compartment model was the best choice for fentanyl, sufentanil and butorphanol. Pharmacokinetic analysis was performed with the PREDPP subroutines ADVAN 11 TRANS 4 (three-compartment model) and ADVAN 3 TRANS 4 (two-compartment model) implemented in NONMEM. For a three compartment model the pharmacokinetic parameters clearance (Cl), inter-compartmental clearances (Q2 and Q3) and the volumes of distribution (V1, V2 and V3) are estimated whereas Q3 and V3 are excluded when using a two-compartment model.

The interanimal variability in the pharmacokinetic parameters was assumed to be log normally distributed:

$$P_i = P_{typ} \cdot \exp(\eta_i) \quad (1)$$

with

$$\eta_i \sim N(0, \omega^2) \quad (2)$$

where  $P_i$  is the individual value of the model parameter  $P$ ,  $P_{typ}$  is the typical value (population value) of parameter  $P$  in the population, and  $\eta_i$  is the realization from a normally distributed inter-animal random variable with mean zero and variance  $\omega^2$ . Inter-animal variability was investigated for each parameter and was fixed to zero when the MVOF did not improve. Correlations between the inter-animal variability of the various parameters were graphically explored.

The residual error, which accounts for unexplained errors (e.g. measurement and experimental errors), in the blood drug concentrations was best described with a proportional error model according to equation:

$$C_{obs,ij} = C_{pred,ij} \cdot (1 + \varepsilon_{ij}) \quad (3)$$

with

$$\varepsilon_{ij} \sim N(0, \sigma^2) \quad (4)$$

Where  $C_{obs,ij}$  is the  $j$ -th observation of the  $i$ -th individual,  $C_{pred,ij}$  is the predicted concentration and  $\varepsilon_{ij}$  is the normally distributed residual random variable with mean zero and variance  $\sigma^2$ .

To refine the pharmacokinetic models, the relationship between bodyweight and the different parameters was explored graphically. The following equation was used to model the parameter as a function of bodyweight ( $BW$ ):

$$P_i = \theta_i + \theta_j \cdot (BW - \text{median}(BW)) \quad (5)$$

where  $P_i$  is the individual value of model parameter  $P$  and  $\theta_i$  and  $\theta_j$  are the intercept and slope of the relationship between the parameter and bodyweight.

The accuracy of the pharmacokinetic was investigated by an internal validation method, the predictive check (Cox *et al.* 1999; Yano *et al.* 2001). With this method, 1000 curves were simulated from the final PK parameter estimates. The median, lower (2.5%) and upper (97.5%) limit of the interquantile range of the simulated concentrations were calculated and compared with the positions of the observations.

Individual pharmacokinetic parameter estimates were used as input for the pharmacodynamic models. Individual blood concentrations were calculated at the times of the EEG measurements.

#### *Biophase distribution models*

In this study, the changes in the delta frequency band of the EEG are used as a measure of drug response. A delay in effect (hysteresis) was observed for all opioids except alfentanil. The hysteresis was characterized on the basis of two biophase distribution models: A) the one-compartment biophase distribution model, also known as the effect-compartment model and B) the extended-catenary biophase distribution model.

#### *A) One-compartment biophase distribution model*

With the one-compartment distribution model, the effect-compartment is linked to the blood concentrations with the rate constant  $k_{1e}$  and the rate constant for drug loss  $k_{eo}$ . The rate of change of the drug concentration in the effect compartment can then be expressed by equation:

$$\frac{dC_e}{dt} = k_{1e} \cdot C_b - k_{eo} \cdot C_e \quad (6)$$

where  $C_b$  represents the blood concentration and  $C_e$  represents the effect-site concentration. Under the assumption that in equilibrium the effect-site concentration equals the blood concentration, this equation can be simplified to:

$$\frac{dC_e}{dt} = k_{eo} \cdot (C_b - C_e) \quad (7)$$

This model describes a symmetrical biophase. In contrast, when  $k_{1e}$  is not equal to  $k_{eo}$ , the biophase is considered to be asymmetrical. For all opioids both models were investigated.

#### *B) Extended-catenary biophase distribution model*

With the extended-catenary biophase distribution model, an extra effect-compartment is added to describe the delay in pharmacological response. The rate of change of the

concentrations in the effect compartments can then be described as follows:

$$\frac{dC_{et}}{dt} = k_{1e} \cdot C_b - k_{1e} \cdot C_{et} \quad (4)$$

$$\frac{dC_e}{dt} = k_{1e} \cdot C_{et} - k_{e0} \cdot C_e \quad (4)$$

where  $C_{et}$  and  $C_{e1}$  describe the concentrations in the transfer and effect-compartment, respectively. The concentrations in the second effect-compartment will then be linked to the pharmacological effect. Both the symmetrical ( $k_{1e}=k_{e0}$ ) and the asymmetrical ( $k_{1e} \neq k_{e0}$ ) biophase models were investigated.

A schematic diagram of the PK-PD models used in the analysis is shown in figure 2.

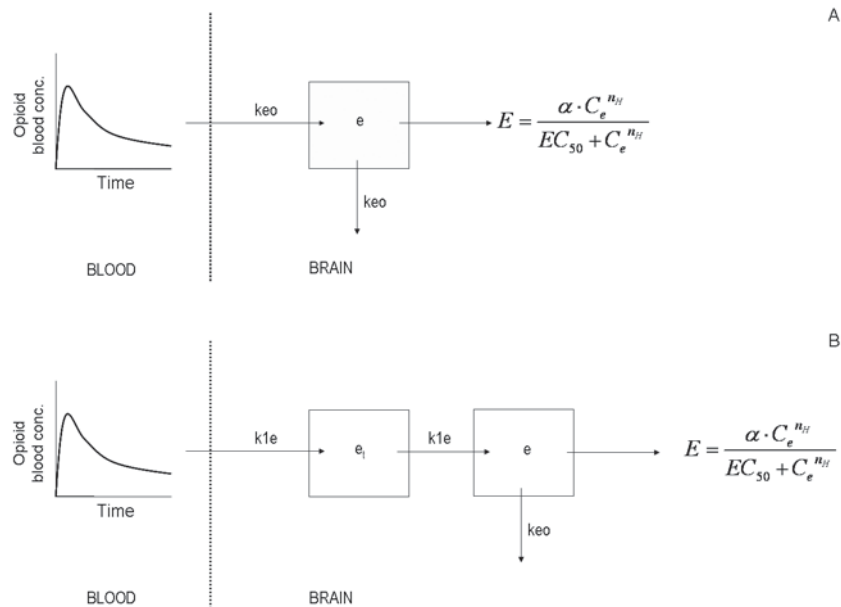


**Figure 2:** A schematic overview of the PK-PD models used in the analysis. Panel A shows the one-compartment biophase distribution, also known as the effect-compartment model, consisting of one effect (e) compartment. Panel B shows the extended catenary biophase distribution model which consists of two sequential effect compartments, the transfer (e<sub>1</sub>) and the effect (e) compartment. The concentrations in the effect compartment were related to the EEG effect (Groenendaal *et al.* 2007 – chapter 6). The blood pharmacokinetics was used as input function.

*PK-PD analysis*

After hysteresis minimization, the individual concentration-effect relationships were fitted simultaneously to the Hill equation:

$$E = E_0 + \frac{\alpha \cdot C^{n_H}}{EC_{50}^{n_H} + C^{n_H}} \quad (10)$$

where  $E_0$  is the no-drug response,  $\alpha$  is the intrinsic activity,  $EC_{50}$  is the potency and  $n_H$  is the slope factor. The stochastic part of the model, used to describe the inter-animal variability in the pharmacodynamic parameters consisted of a proportional error model for  $E_0$  and  $\alpha$  (equation 11) and an exponential error model for  $EC_{50}$  (equation 1).

$$P_i = P_{typ} \cdot (1 + \eta_i) \quad (11)$$

with

$$\eta_i \sim N(0, \omega^2) \quad (11)$$

Similar to the pharmacokinetics, the residual error in the pharmacodynamics could be best described with a proportional error model according to equation 6. The accuracy of the pharmacodynamic models was investigated by an internal validation method, the predictive check as explained for the pharmacokinetics.

*In vitro transport characteristics*

The interaction with Pgp and the apparent membrane permeability ( $P_{app}$ ) were determined *in vitro* using monolayers of MDCK:MDR1 cells. The cells were cultured in DMEM – glutamax media, formulated with D-glucose (4.5 g/l), L-alanyl-glutamine and phenol red and supplemented with penicillin (10000 U/ml)-streptomycin (10000 µg/ml) and 10% (v/v) fetal calf serum at 37 °C and 5% CO<sub>2</sub>. Cells were trypsinized every 4 days. For the studies, cells were seeded onto BD Falcon™ HTS 24-Multiwell Inserts at a seeding density of 50000 cells/well and grown for 3 days in DMEM full media.

Before each experiment, transepithelial electrical resistance was measured with an EVOM™ voltohmmeter (World Precision Instruments, Stevenage, United Kingdom). The experiments were performed in transport buffer (DMEM containing 25 mM HEPES without phenol red and sodium pyruvate). Cells were pre-incubated with transport buffer containing GF120918 (2 µM) or vehicle (0.5% DMSO) for 15 min at 37°C. After removal of pre-incubation solutions, the test solutions were added and the cells were incubated for 90 min at 37°C under continuous shaking. Donor test solutions contained DMSO or GF120918, lucifer yellow (10 µM) and opioid (3 µM) or amprenavir (3 µM). Receiver test solutions were identical to the pre-incubation solutions. All experiments were performed automatically using the robotic TECAN™ genesis workstation (TECAN, Reading, United Kingdom). Reference drugs for paracellular transport (lucifer yellow) and Pgp-efflux (amprenavir) were included in each experiment to test the integrity and quality of the monolayer. After 90 min of incubation, 100 µl samples were

collected to determine lucifer yellow, amprenavir and test compound concentrations. Transport was measured in two directions: apical-to-basolateral (a→b) and basolateral-to-apical (b→a) and in duplicate.

Alfentanil, fentanyl, sufentanil and butorphanol were analysed by dual high-performance liquid chromatography with tandem mass spectrometry (LC/MS/MS). The system consisted of an API-365 (Applied Biosystems, Warrington, United Kingdom) LC/MS/MS employing positive ion turbospray ionisation with a CTC HTS PAL autosampler (CTC Analytics, Hitchin, United Kingdom). Chromatography was conducted on a 50 mm x 2.1 mm HypURITY column (ThermoHypersil, Runcorn, United Kingdom) at a flow rate of 0.8 ml/min and a split ratio of 1:2. The mobile phase consisted of two solvents: (A) 10 mM ammonium acetate pH 4 and (B) 100% acetonitrile. The gradient profile was at 0 min 80% A and 20% B, at 1 min 0% A and 100% B and at 1.1 min 80% A and 20% B. Total run time was 1.5 min. Data acquisition was performed with PE Sciex version 1.1 (Applied biosystems, Warrington, United Kingdom) and data were reported at the ratio of test compound peak area over internal standard peak area.

Nalbuphine and morphine samples were analysed by high performance liquid chromatography with electrochemical detection (HPLC-ECD) as described above for the samples from the PK-PD studies.

Lucifer yellow samples were analysed by a Polarstar® fluorescence microplate reader with  $\lambda_{ex}$ =430 nm and  $\lambda_{em}$ =538 nm (BMG-Labtech, Aylesbury, United Kingdom).

The efflux ratio was calculated by dividing the amount transported from basolateral to apical (b→a) by the amount transported from apical to basolateral (a→b). Involvement of Pgp mediated efflux was identified if the efflux ratio was >1.5 (Mahar Doan *et al.* 2002). To confirm that efflux was due to Pgp-mediated transport, the efflux ratio was also determined in the presence of the Pgp inhibitor GF120918. In the presence of GF120918, the efflux ratio should decrease to 1. The apparent permeability of the compounds was calculated using the equation:

$$P_{app} = -\left(\frac{V_R \cdot V_D}{(V_R + V_D) \cdot A \cdot t}\right) \cdot \ln\left\{1 - \frac{CR(t)}{\langle C(t) \rangle}\right\} \quad (13)$$

where  $P_{app}$  represents the apparent permeability in nm/sec,  $V_D$  and  $V_R$  are the donor and receiver chamber volumes (cm<sup>3</sup>),  $A$  is the area of the permeability barrier (cm<sup>2</sup>),  $t$  is the time of the measurements (s),  $C_R(t)$  is the drug concentration in the receiver chamber and  $\langle C(t) \rangle$  is described by equation 11.

$$\langle C(t) \rangle = \frac{V_D \cdot C_D(t) + V_R \cdot C_R(t)}{V_D + V_R} \quad (14)$$

where  $\langle C(t) \rangle$  describes the average system concentration,  $V_D$  and  $V_R$  are the donor and receiver chamber volumes (cm<sup>3</sup>) and  $C_D(t)$  and  $C_R(t)$  are the donor and receiver



concentrations at time  $t$  (Tran *et al.* 2004; 2005).

In all studies, amprenavir efflux ratios, apparent permeability of lucifer yellow and mass balance were used as controls. The mass balance was calculated using the equation:

$$\%MB = \frac{A_{rt} + A_{dt}}{A_{d0}} \cdot 100 \quad (15)$$

where %MB is the mass balance,  $A_{rt}$  is the drug amount in receiver chamber at time ( $t$ ),  $A_{dt}$  is the drug amount in donor chamber at time ( $t$ ) and  $A_{d0}$  is the drug amount in the donor chamber at  $t=0$ . This calculation of  $P_{app}$  takes into account the loss of drug from the donor compartment, which results in a better estimation of the  $P_{app}$ .

Experiments were only included when efflux ratio of amprenavir > 16 and when apparent permeability of lucifer yellow < 50 nm/sec and mass balance > 70 %.

#### *Quantitative structure activity relationships – physico-chemical relationships*

Log octanol/water partition coefficients (cLogP) was calculated using Daylight Software v4.71/82 (Daylight Chemical Information Systems Inc., Irvine, CA). Polar surface areas (PSA) were calculated according to Ertl and co-workers (2000). A predictor of BBB transport characteristics was also determined based on the Abraham equation (Abraham *et al.* 1994):

$$\text{LogBB} = -0.038 + 0.198 \cdot R_2 - 0.687 \cdot \pi_2^H - 0.715 \cdot \alpha_2^H - 0.698 \cdot \beta_2^H + 0.995 \cdot V_x \quad (16)$$

where LogBB is the logarithm of the blood-brain concentration ratio and  $R_2$ ,  $\pi_2^H$ ,  $\alpha_2^H$ ,  $\beta_2^H$  and  $V_x$  are defined as the excess molar refractivity, dipolarity/polarisability, hydrogen bond acidity, hydrogen bond basicity and the solute McGowan volume, respectively, as described by Platts and co-workers (Platts *et al.* 1999).

#### *Statistical analysis*

The *in vitro* data were analysed using an unpaired Student's t-test (two-tailed) or one-way analysis of variance (ANOVA) (Graphpad Instat® version 3.00). A value of  $p < 0.05$  was considered a significant difference. All data are expressed as mean  $\pm$  SEM, unless indicated otherwise. Each experiment was performed at least three times. Linear regression analysis of *in vivo*  $k_{le}$  with the *in vitro*  $P_{app}$  and the physicochemical properties (cLogP, PSA, LogBB) were performed in S-plus 6.0 professional, release 1 (Insightful corporation, USA) using a confidence level of 0.95 and no weight factor.

RESULTS

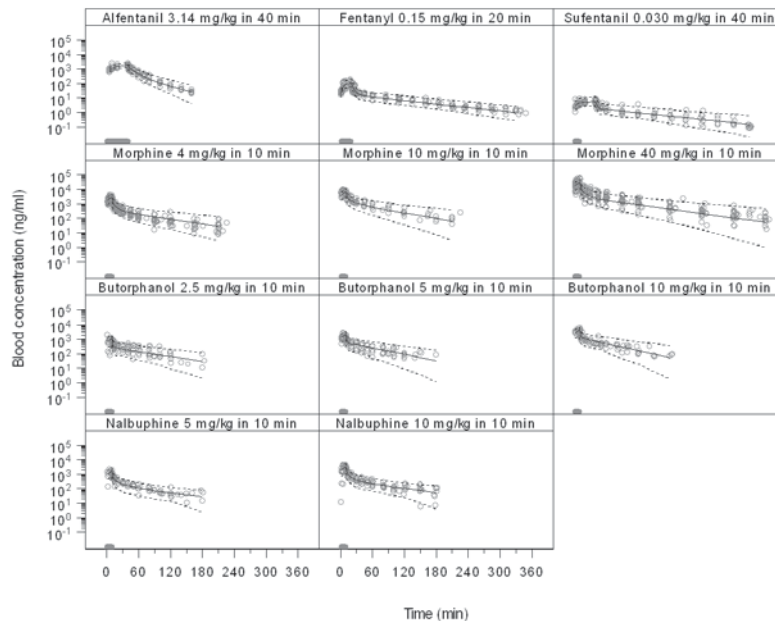
*Pharmacokinetics*

Figure 3 shows the observed, population predicted and 2.5% and 97.5% quantiles for 3.14 mg/kg alfentanil in 40 min, 0.15 mg/kg fentanyl in 20 min, 0.030 mg/kg sufentanil in 40 min, 4/10/40 mg/kg morphine in 10 min, butorphanol 2.5/5/10 mg/kg in 10 min and nalbuphine 5/10 mg/kg in 10 min. The pharmacokinetics of fentanyl, sufentanil and butorphanol were best described with a two-compartment model, whereas a three-compartment pharmacokinetic model was used for alfentanil, morphine and nalbuphine. All parameters were estimated accurately as shown in table 2. Covariate analysis showed a linear relationship between bodyweight and CL for fentanyl, a linear relationship between bodyweight and V2 for butorphanol and linear relationships between bodyweight and CL and bodyweight and V2 for morphine. No individual differences in posthoc values were found between the different dosages of morphine, butorphanol and nalbuphine. Between the opioids, differences were observed between the pharmacokinetic parameter values, especially for the volume of the peripheral compartments (V2+V3), ranging from 175 to 1845 ml for alfentanil and nalbuphine, respectively.

**Table 2:** Population blood pharmacokinetic parameter estimates and standard error of estimate (mean ± SE) for C<sub>1</sub>, V<sub>1</sub>, Q<sub>2</sub>, V<sub>2</sub>, Q<sub>3</sub> and V<sub>3</sub>. The variances (ω<sup>2</sup>) describing the inter-individual variability are shown in parentheses.

Compound	Cl (ml/min)	V1 (ml)	Q2 (ml/min)	V2 (ml)	Q3 (ml/min)	V3 (ml)
Morphine	20.8 ± 1.2 -0.13	68 ± 11 (--)	15.5 ± 1.8 (--)	739 ± 56 -0.1	17.8 ± 3.3 (--)	133 ± 21 (--)
Alfentanil	10.0 ± 0.8 -0.03	19 ± 5 (--)	22.9 ± 2.6 (--)	111 ± 10 -0.01	1.97 ± 0.3 (--)	64 ± 14 -0.06
Fentanyl	11.5 ± 1.2 -0.02	98 ± 9 (--)	11.4 ± 2.8 (--)	586 ± 94 -0.03	-- (--)	-- (--)
Sufentanil	20.6 ± 2.7 -0.07	113 ± 42 (--)	31.2 ± 3.6 (--)	1370 ± 204 -0.06	-- (--)	-- (--)
Butorphanol	22.9 ± 2.3 -0.14	81 ± 23 (--)	58.8 ± 5.9 (--)	1030 ± 89 -0.09	-- (--)	-- (--)
Nalbuphine	39.0 ± 3.0 -0.04	130 ± 29 (--)	37.8 ± 4.7 (--)	1580 ± 294 -0.34	44.2 ± 12.4 (--)	265 ± 74 -0.27

The accuracy of the models was investigated using the predictive check. The selected PK models could well predict the time course of the opioids after intravenous infusion as shown in figure 3.



**Figure 3:** Blood pharmacokinetics of the opioids. Observed (grey dots), population predicted (solid line) and 2.5% and 97.5% quantiles (dotted lines) are depicted for each individual opioid per dose. The name of the compound and the dose are depicted at the top of each panel. Time in minutes is depicted on the x-axis and the blood concentration is depicted on the y-axis on a logarithmic scale. The grey bar indicates the infusion time.

#### *Pharmacodynamics and hysteresis*

After start of the opioid infusion, a gradual increase in EEG effect was observed, expressed as absolute amplitude in the 0.5-4.5 Hz frequency range. Large differences in onset of the effect and maximum effect were observed between the opioids (figures 4 and 5). For example, for alfentanil the maximum effect was observed at the end of the infusion, whereas for morphine, the maximal effect was observed around 20 minutes after the end of the infusion. The maximum effect ( $\alpha$ ) of alfentanil and sufentanil were around 100  $\mu$ V, whereas for fentanyl, morphine, butorphanol and nalbuphine and butorphanol the maximum effect was 78, 45, 57 and 18  $\mu$ V, respectively. Duration of the effect (from the start of the infusion until the return to baseline values) was around 180 minutes for alfentanil, 4 and 10 mg/kg morphine, all doses of butorphanol and nalbuphine, whereas for fentanyl, sufentanil and 40 mg/kg morphine, the duration of the effect was around 360 min. The baseline values for alfentanil, fentanyl and

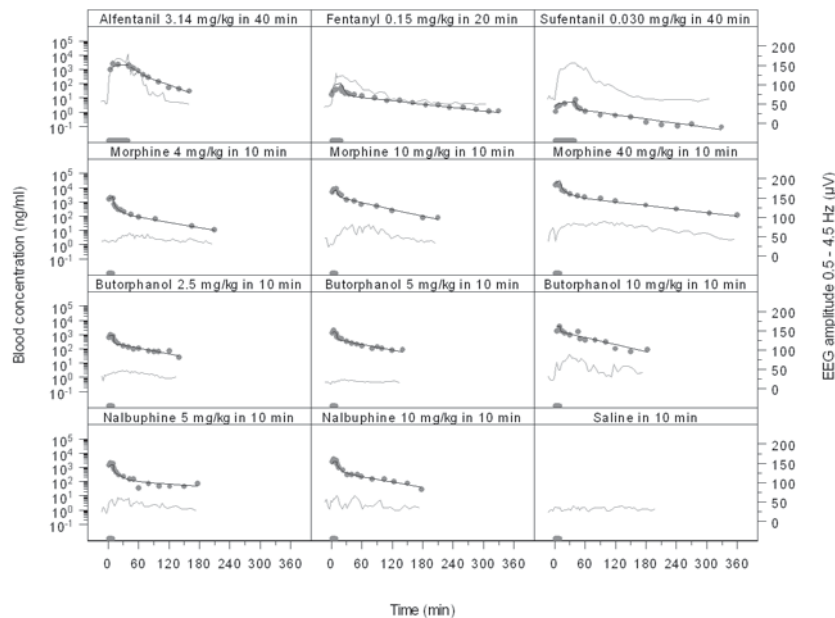


**Figure 4:** Blood pharmacokinetics and EEG effect (pharmacodynamics) of a typical rat after administration of the opioids. Observed concentrations (grey dots), individual predicted concentrations (black line) and observed effect are depicted for each individual opioid per dose. The grey bar indicates the infusion time. Time in minutes is depicted on the x-axis, the blood concentration is depicted on the left y-axis on a logarithmic scale and the effect as EEG amplitude in the d-frequency range is depicted on the right y-axis on a linear scale. The name of the compound and the dose are depicted at the top of each panel.

sufentanil were significantly higher than the baseline values for morphine, butorphanol and nalbuphine. This is probably caused by differences in surgical and experimental conditions, since the data for alfentanil, fentanyl and sufentanil have been collected and published previously (Cox *et al.* 1998). Validation experiments with fentanyl indicated that a difference in baseline does not affect the actual effect-time profile and maximal effect (data not shown).

The individual pharmacokinetic parameters were used to calculate the blood concentrations at the time points of the individual EEG measurements. The derived concentration-effect relationships showed hysteresis for all opioids, except alfentanil. For each opioid and each dose the concentration-effect relationships are shown in figure 5.

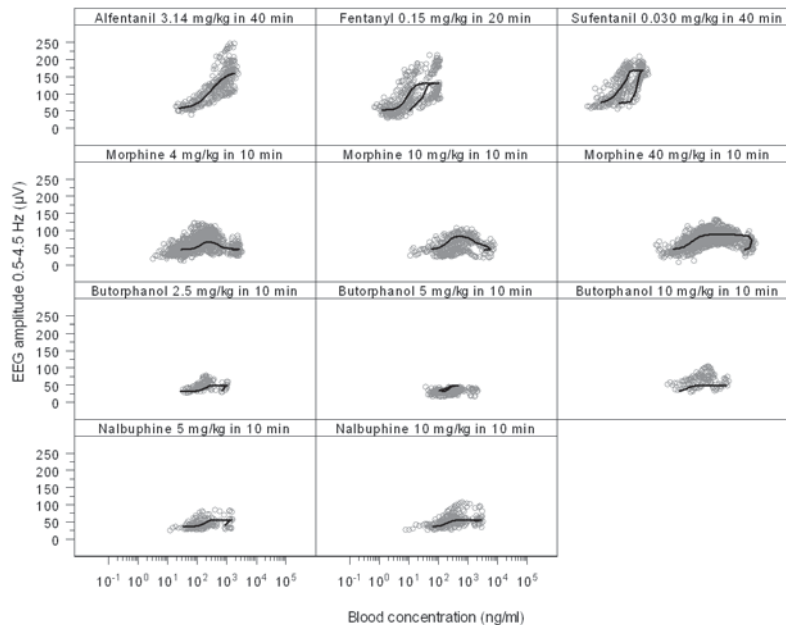


**Figure 5:** The PK-PD relationship after administration of the opioids. Observed (grey dots) and individual predictions (black line) are depicted for each individual opioid per dose. Blood concentrations are depicted on the x-axis on a logarithmic scale and the EEG amplitude in the  $\delta$ -frequency range is depicted on the y-axis on a linear scale. A hysteresis loop was observed for all opioids, except alfentanil.

#### Biophase distribution models

Both the one-compartment distribution model and the extended-catenary biophase distribution model were investigated for all opioids except alfentanil, including the symmetrical and a-symmetrical biophase distribution kinetics. A summary of the goodness-of-fit of the four biophase distribution models is shown in table 3. For morphine the extended-catenary biophase distribution model best described the biophase distribution kinetics as has been shown previously (Groenendaal *et al.*, 2007 – chapter 6). In contrast, for fentanyl, sufentanil, nalbuphine and butorphanol, the symmetrical one-compartment biophase distribution model best described the transport to the effect-site. A-symmetrical biophase distribution kinetics could not be identified for the opioids except for morphine. Analysis with the extended-catenary biophase distribution model resulted in an increase in minimum value of objective function or did not result in successful minimization. The  $k_{1e}$  values for transport to the effect-site (is equal to  $k_{e0}$  except for morphine) ranged from  $0.47 \text{ min}^{-1}$  ( $t_{1/2,k1e} = 1.45 \text{ min}$ ) for fentanyl to  $0.04 \text{ min}^{-1}$  ( $t_{1/2,k1e} = 17.3 \text{ min}$ ) for morphine (table 5). Based on the  $k1e$  values the following range in distribution kinetics could be identified: alfentanil (value close to infinity) > fentanyl ( $0.47 \text{ min}^{-1}$ ) > butorphanol ( $0.21 \text{ min}^{-1}$ ) > nalbuphine ( $0.20 \text{ min}^{-1}$ ) > sufentanil ( $0.17 \text{ min}^{-1}$ ) > morphine ( $0.04 \text{ min}^{-1}$ ).

**Table 3:** Summary of goodness-of-fit based on the minimum value of objective function, of four biophase distribution models containing expressions for transport to the effect-site and loss from the effect site. This models include the symmetrical ( $k_{1e}=k_{e0}$ ) and a-symmetrical ( $k_{1e}\neq k_{e0}$ ) extended-catenary biophase distribution model and the symmetrical ( $k_{1e}=k_{e0}$ ) and a-symmetrical ( $k_{1e}\neq k_{e0}$ ) one-compartment distribution model.

Compound	One-compartment biophase distribution model		Extended-catenary biophase distribution model	
	$k_{1e}=k_{e0}$	$k_{1e}\neq k_{e0}$	$k_{1e}=k_{e0}$	$k_{1e}\neq k_{e0}$
	Morphine	m.t.	25234	24936
Fentanyl	2497	2497	2504	m.t.
Sufentanil	2297	2298	2324	m.t.
Butorphanol	2542	2542	2620	m.t.
Nalbuphine	2796	2796	2793	2793

Abbreviations: m.t.= minimization terminated

Note: alfentanil is not included in this analysis since no hysteresis was observed.

#### PK-PD analysis

After hysteresis minimization, the effect site (biophase) concentration-effect relationships were analysed with the Hill equation (equation 3), resulting in estimates for baseline ( $E_0$ ), intrinsic activity ( $\alpha$ ), potency ( $EC_{50}$ ) and slope ( $n^H$ ). The effect-site concentration-effect relationship of each opioid is shown in figure 6. The highest intrinsic activity was found for alfentanil (109  $\mu V$ ) and the lowest for butorphanol (18  $\mu V$ ). Based on the intrinsic activity, the following range of agonism could be identified: alfentanil (109  $\mu V$ ) > sufentanil (99  $\mu V$ ) > fentanyl (78  $\mu V$ ) > nalbuphine (57  $\mu V$ ) > morphine (45  $\mu V$ ) > butorphanol (18  $\mu V$ ). The estimated pharmacodynamic parameters are shown in table 4.

#### In vitro transport characteristics and QSAR modeling

The *in vitro* transport characteristics of the opioids were investigated in MDCK:MDR1 cells expressing the human Pgp. Substrate assessment studies were performed to identify Pgp substrates and to calculate the  $P_{app}$  value, a measure of the passive membrane transport.

No statistically significant differences were found in the Pgp substrate efflux ratios for alfentanil, fentanyl, sufentanil and butorphanol in the presence or absence of GF120918. For morphine and nalbuphine the concentrations in the receiver compartment were below the limit of quantification of the assay when using the donor concentration of 3  $\mu M$ . However, at a donor concentration of 100  $\mu M$  morphine was identified as a Pgp substrate. For nalbuphine literature values were used (Mahar Doan, Humphreys *et al.* 2002). At a donor concentration of 10  $\mu M$ , nalbuphine was identified as a Pgp substrate. The experimental settings used by Mahar Doan and co-workers were similar to the

**Table 4:** Population pharmacodynamic estimates and standard error of estimate (mean  $\pm$  SE) for, intrinsic activity ( $\alpha$ ), potency ( $EC_{50}$ ), Hill slope ( $n_H$ ) and baseline ( $E_0$ ). The variances ( $\omega^2$ ) describing the inter-individual variability are shown in parentheses.

Compound	$k_{1e}$ ( $\text{min}^{-1}$ )	$k_{e0}$ ( $\text{min}^{-1}$ )	$E_0$ ( $\mu\text{V}$ )	$\alpha$ ( $\mu\text{V}$ )	$EC_{50}$ (ng/ml)	$n_H$
Morphine	$0.038 \pm 0.003$	$0.043 \pm 0.003$	$45 \pm 1$	$45 \pm 4$	$451 \pm 78$	$2.3 \pm 0.2$
		-0.24	-0.03	-0.12	(-)	(-)
Alfentanil	--	--	$56 \pm 2$	$109 \pm 13$	$303 \pm 56$	$1.6 \pm 0.2$
			-0.01	-0.11	-0.16	(-)
Fentanyl	$0.47 \pm 0.10$	$0.47 \pm 0.10$	$53 \pm 4$	$78 \pm 9$	$8.9 \pm 0.8$	$3.2 \pm 0.3$
			-0.06	-0.11	-0.04	(-)
Sufentanil	$0.17 \pm 0.05$	$0.17 \pm 0.05$	$72 \pm 4$	$99 \pm 8$	$1.2 \pm 0.2$	$2.1 \pm 0.4$
			-0.02	-0.02	-0.21	(-)
Butorphanol	$0.21 \pm 0.03$	$0.21 \pm 0.03$	$32 \pm 2$	$18 \pm 4$	$195 \pm 34$	$4.1 \pm 0.8$
			-0.05	-0.73	-0.36	(-)
Nalbuphine	$0.20 \pm 0.04$	$0.20 \pm 0.04$	$37 \pm 2$	$57 \pm 4$	$205 \pm 24$	$3.4 \pm 0.6$
			-0.03	-0.07	-0.15	(-)

Note: For morphine the extended catenary biophase distribution model was used to describe the biophase distribution, for fentanyl, sufentanil, butorphanol and nalbuphine the one-compartment distribution model was used, whereas no hysteresis was observed for alfentanil.

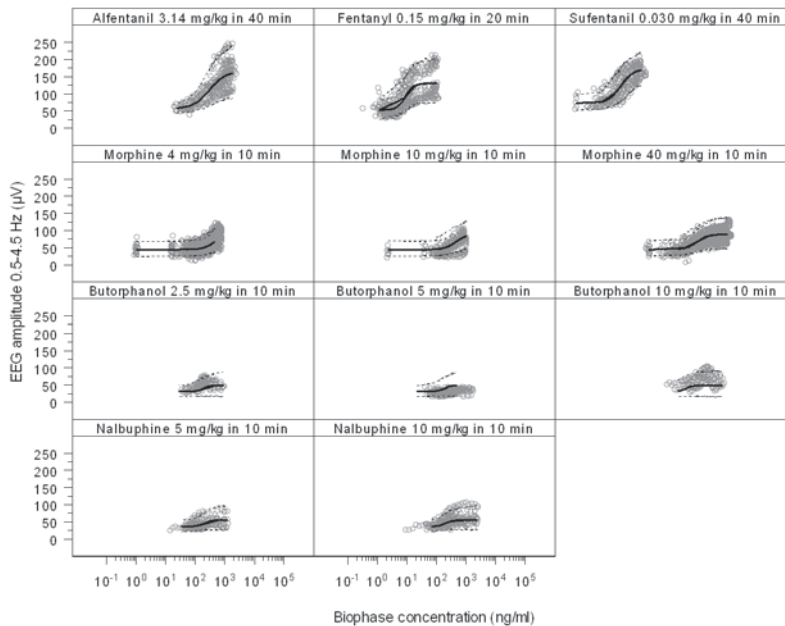


**Figure 6:** PK-PD relationships of the opioids after hysteresis minimisation. Observed (grey dots), population predicted (solid line) and 2.5% and 97.5% quantiles (dotted lines) are depicted for each individual opioid per dose. The name of the compound is depicted at the top of each panel. The predicted lines were obtained using the effect-compartment model with the Hill equation.

ones used in the present investigation and therefore the use of literature values was justified.

The  $P_{app}$  values of the opioids were calculated on the basis of the amount transported across the monolayer over time (nm/s), in both directions, in the presence of GF120918.  $P_{app}$  values > 500 nm/s were found for alfentanil, fentanyl, sufentanil and butorphanol, whereas the  $P_{app}$  values of nalbuphine and loperamide were 156 and 206 nm/s, respectively. For morphine, the  $P_{app}$  value was 16 nm/s, indicating that almost no morphine is transported across the monolayer within the experimental period of 90 min.

The efflux ratios in the absence and presence of GF120918, the  $P_{app}$  values and the calculated cLogP, logBB and PSA are listed in table 5.

**Table 5:** Results of the *in vitro* transport studies in MDCK:MDR1 cells and physico-chemical properties. *In vitro* studies: averaged (mean  $\pm$  SEM, n=3) estimate of efflux ratio (transport b  $\rightarrow$  a / transport a  $\rightarrow$  b) and apparent permeability ( $P_{app}$ ). Each determination was carried out in duplicate. For nalbuphine literature values were used (Mahar Doan et al. 2002). The efflux ratio was determined at a donor concentration of 3  $\mu$ M, except for nalbuphine

Compound	Efflux ratio		$P_{app}$ (nm/sec)	cLogP	LogBB	PSA ( $\text{\AA}$ )
	Buffer	GF120918				
Morphine	4.1	n.d.	16	0.6	-0.28	52.9
Alfentanil	0.83 $\pm$ 0.05	1.05 $\pm$ 0.11	698 $\pm$ 39	2.1	0.277	85.5
Fentanyl	0.72 $\pm$ 0.07	0.81 $\pm$ 0.07	728 $\pm$ 105	3.6	0.886	23.6
Sufentanil	1.09 $\pm$ 0.39	0.76 $\pm$ 0.07	590 $\pm$ 42	3.6	0.932	32.8
Butorphanol	0.61 $\pm$ 0.10	0.74 $\pm$ 0.14	779 $\pm$ 48	3.7	0.253	43.7
Nalbuphine	2.17	1.01	156 $\pm$ 0.1	1.4	-0.247	73.2

Abbreviations: cLogP – calculated LogP value, which is indicative for lipophilicity, LogBB - BBB transport on basis of Abraham equation, PSA - polar surface area ( $\text{\AA}$ ) and n.d. – not determined.

#### *In vitro/in silico/in vivo correlations*

Regression analysis was performed to investigate the possible correlations between the *in vivo*  $k_{le}$  and the *in vitro*  $P_{app}$  and the *in vivo*  $k_{le}$  with the physico-chemical properties of the selected opioids. The results are shown in figure 7. For all opioids except morphine, the  $k_{le}$  was equal to the  $k_{eo}$ . For morphine the  $k_{le}$  was estimated separately. A significant correlation was found between the *in vitro*  $P_{app}$  and the *in vivo*  $k_{le}$ , which could be described on the basis of:  $k_{le} = 0.13 * \log P_{app} - 0.09$ . For physicochemical properties, no significant correlations could be identified.



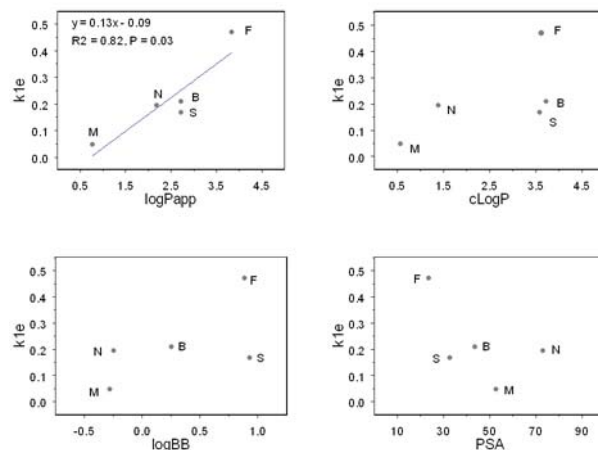


**Figure 7:** Correlation between the  $k_{1e}$  and the  $P_{app}$  and the  $k_{1e}$  and the physicochemical properties of the opioids. The compounds are depicted with the first letter of the opioid name.

## DISCUSSION

The objectives of the study presented here were to study the biophase distribution kinetics in the PK-PD correlation of a wide range of opioids. Previously, the biophase distribution kinetics of morphine have been investigated in the rat EEG model, which were best described with the extended-catenary biophase distribution model. This model consists of two sequential effect compartments (i.e. a shallow and a deep effect compartment) and two rate constants for transport through the transfer compartment ( $k_{1e}$ ) and for loss from the effect compartment ( $k_{e0}$ ) (Groenendaal *et al.*, 2007 - chapter 6). Morphine behaved as a low efficacy agonist with an intrinsic activity of 44.5  $\mu V$ . It was of interest to extend the investigations on the biophase distribution kinetics for a wide range of opioids. In the current study, two biophase distribution models were investigated, with respect to intrinsic activity and onset of the EEG effect: 1) the one-compartment biophase distribution model (the effect-compartment model) and 2) the extended-catenary biophase distribution model. The predicted biophase concentrations were related to the EEG effect on the basis of the sigmoidal Emax pharmacodynamic model. In addition, *in vitro* and *in silico* studies were also included to investigate the membrane transport characteristics of opioids with respect to P-glycoprotein interaction, apparent membrane permeability and physico-chemical properties.

### Pharmacokinetics

The pharmacokinetics of all opioids could be successfully described using population PK analysis. For fentanyl, sufentanil and butorphanol, a two-compartment model

best described the data whereas for alfentanil, morphine and nalbuphine a three-compartment model was most suitable. Previously, Cox and co-workers used a two-compartment model to describe the pharmacokinetics of alfentanil (1997; 1998). However, in the present analysis a population approach was used for the analysis whereas Cox and co-workers analyzed the data per individual. With a population approach both intra- and inter-individual variability are taken into account, thereby increasing the power of the models. All pharmacokinetic parameters could be accurately estimated as shown in table 2. Internal validation with the predictive check confirmed the accuracy of the pharmacokinetic models. Differences were found in the pharmacokinetic characteristics of the opioids, especially in the volume of distribution of the peripheral compartments. For alfentanil a total peripheral volume of 175 ml was found in contrast to nalbuphine where a total peripheral volume of 1845 ml was observed, indicating the butorphanol is widely distributed into tissues compared to alfentanil. The clearance values ranged from 10 ml/min for alfentanil to 39 ml/min for nalbuphine.

#### *Biophase distribution models*

Both the one-compartment distribution model and the extended-catenary biophase distribution model were investigated for all opioids, including the symmetrical and asymmetrical biophase distribution kinetics. The concentration-effect profiles (figure 5) revealed that for all opioids except alfentanil, a delay in effect was observed. Therefore, for alfentanil no distribution models were tested. The biophase distribution kinetics of morphine were best described with the extended-catenary biophase distribution model as shown previously (Groenendaal *et al.*, 2007 – chapter 6), with different values for  $k_{1e}$  and  $k_{e0}$  (asymmetrical biophase). When the data from the rats co-infused with GF120918 were removed from the analysis, the asymmetrical biophase distribution could still be identified. The values for  $k_{1e}$  and  $k_{e0}$  were  $0.038 \text{ min}^{-1}$  and  $0.043 \text{ min}^{-1}$ , respectively. Simplification to the asymmetrical model resulted in a significant increase in objective function and a significant worsening of the fit.

The symmetrical one-compartment biophase distribution model, where  $k_{1e} = k_{e0}$ , yielded the most accurate parameter estimates for the biophase distribution kinetics of fentanyl, sufentanil and butorphanol. The use of the asymmetrical one-compartment biophase model did not result in an improvement of the accuracy of the parameters, while no parameter estimates could be obtained when using the extended-catenary biophase distribution model. These findings were expected since the delay in the EEG effect was relatively short, as is confirmed by the  $k_{1e}$  values of  $0.47 \text{ min}^{-1}$ ,  $0.17 \text{ min}^{-1}$  and  $0.21 \text{ min}^{-1}$  for fentanyl, sufentanil and butorphanol, respectively. For nalbuphine, a small increase of 2 points in objective function was observed when the biophase distribution was simplified from the extended-biophase distribution model to the one-compartment distribution model. The accuracy of the parameter estimates did not improve and therefore, it was concluded that the simplest model, the one-compartment model was most appropriate to describe the biophase distribution kinetics of nalbuphine. In

addition, asymmetrical distribution could not be identified for nalbuphine and the estimated  $k_{1e}$  (and  $k_{e0}$ ) value was  $0.20 \text{ min}^{-1}$ .

#### *PK-PD analysis*

The differences in intrinsic activity were shown by the PK-PD analysis with the empirical Hill equation. Alfentanil, fentanyl and sufentanil behaved as high efficacy agonists and all displayed the same intrinsic activity of around  $100 \mu\text{V}$ , although the intrinsic activity of fentanyl was slightly lower ( $78 \mu\text{V}$ ). Morphine, butorphanol and nalbuphine had an intrinsic activity of 45, 18 and  $57 \mu\text{V}$ , respectively, and could therefore be classified as low efficacy agonists. Only small differences were observed in parameter estimates when compared to the paper by Cox and co-workers (1998) indicating that estimation of the inter-animal variability in the population approach and the difference in the pharmacokinetic model for alfentanil does not significantly influence the outcome of the PK-PD modelling. Furthermore, it should be mentioned that the estimation of the pharmacodynamic parameters of butorphanol was difficult, because the changes in EEG amplitude were only marginal compared to the baseline EEG taking into consideration the noise in the EEG signal. This is reflected in the inter-animal variability for the intrinsic activity of butorphanol. For all the opioids this value is around 0.1 whereas for butorphanol this value is 0.73 suggesting that the model has difficulties estimating the intrinsic activity. The EEG effects of butorphanol have the lowest intrinsic activity and the estimate for the Hill factor of 4.1 suggests an on-off response.

#### *In vitro transport characteristics and QSAR modelling*

*In vitro* studies were performed to investigate the contribution of Pgp and  $P_{app}$  in transport to the effect site. Morphine and nalbuphine were identified as Pgp substrates whereas for the other opioids, alfentanil, fentanyl, sufentanil and butorphanol, no Pgp-mediated transport was identified. The results were in accordance with literature (Wandel *et al.* 2002). Furthermore, it was shown that the  $P_{app}$  in the presence of GF120918 of alfentanil, fentanyl, sufentanil and butorphanol ( $> 500 \text{ nm/sec}$ ) was much higher compared to nalbuphine ( $156 \text{ nm/sec}$ ) and in particular for morphine with a calculated  $P_{app}$  of only  $16 \text{ nm/sec}$ . The  $P_{app}$  values of  $<50$ ,  $50\text{-}250$ ,  $>250 \text{ nm/sec}$  were considered as low, moderate and high, respectively. These results indicate that transport to the biophase will not be rate-limiting for alfentanil, fentanyl, sufentanil and butorphanol, due to their very high passive permeabilities, while it should be taken into account for nalbuphine and especially morphine.

For the opioids, to investigate the predictability of the *in vivo* results based on *in vitro* and *in silico* data, a regression analysis was performed to specifically test the correlations between the *in vivo*  $k_{1e}$  and the *in vitro*  $P_{app}$  and that between the *in vivo*  $k_{1e}$  and the physico-chemical properties as determined *in silico*. The physicochemical properties that were investigated are cLogP, logBB and PSA. cLogP is a measure for lipophilicity

of the compound,  $\log_{BB}$  is a prediction of the transport characteristics across the BBB, whereas PSA represent the area (size) of the compound. A significant correlation was found between the  $k_{ie}$  and the passive permeability which could be described on the basis of:  $k_{ie} = 0.13 \cdot \log P_{app} - 0.09$  ( $R^2 = 0.83$ ,  $P=0.03$ ). No significant correlations could be identified between the  $k_{ie}$  and the physico-chemical properties, although some trends were observed. Probably, the number of opioids was too limited and moreover these opioids could be divided into two structurally different groups (figure 1). It is therefore expected that the correlations will improve upon inclusion of more opioids. However, based on currently available data, it is concluded that in the *in vitro*  $P_{app}$  is a better predictor for the *in vivo*  $k_{ie}$  than were the physico-chemical properties. However, it should be taken into consideration that processes other the BBB transport, such as distribution within the brain, can also have an impact on the biophase distribution kinetics (Liu *et al.* 2005).

It is concluded that within the wide range of opioids used in this study, only morphine displays complex biophase distribution kinetics, which can be explained by its relatively low passive permeability and the interaction with active transporters at the blood-brain barrier.

#### ACKNOWLEDGEMENTS

The authors gratefully acknowledge the technical assistance M.C.M. Blom-Rosemalen, S.M. Bos-van Maastricht and P. Looijmans.

## REFERENCES

- Abraham MH, Chadha HS, Mitchell RC (1994) Hydrogen bonding. 33. Factors that influence the distribution of solutes between blood and brain. *J.Pharm.Sci.* **83**: 1257-1268
- Beal SL, Sheiner LB (1999) *NONMEM users guide* San Francisco, CA
- Cox EH, Kerbusch T, van der Graaf PH, Danhof M (1998) Pharmacokinetic-pharmacodynamic modeling of the electroencephalogram effect of synthetic opioids in the rat: correlation with the interaction at the mu-opioid receptor. *J Pharmacol.Exp. Ther.* **284**: 1095-1103
- Cox EH, Van Hemert JG, Tukker EJ, Danhof M (1997) Pharmacokinetic-pharmacodynamic modelling of the EEG effect of alfentanil in rats. *J Pharmacol.Toxicol.Methods* **38**: 99-108
- Cox EH, Veyrat-Follet C, Beal SL, Fuseau E, Kenkare S, Sheiner LB (1999) A population pharmacokinetic-pharmacodynamic analysis of repeated measures time-to-event pharmacodynamic responses: the antiemetic effect of ondansetron. *J.Pharmacokinet.Biopharm.* **27**: 625-644
- Dagenais C, Graff CL, Pollack GM (2004) Variable modulation of opioid brain uptake by P-glycoprotein in mice. *Biochem Pharmacol* **67**: 269-276
- Emmerson PJ, Clark MJ, Mansour A, Akil H, Woods JH, Medzihradsky F (1996) Characterization of opioid agonist efficacy in a C6 glioma cell line expressing the mu opioid receptor. *J.Pharmacol.Exp. Ther.* **278**: 1121-1127
- Ertl P, Rohde B, Selzer P (2000) Fast calculation of molecular polar surface area as a sum of fragment-based contributions and its application to the prediction of drug transport properties. *Journal of Medicinal Chemistry* **43**: 3714-3717
- Groenendaal D, Blom-Roosemalen MC, Danhof M, Lange EC (2005) High-performance liquid chromatography of nalbuphine, butorphanol and morphine in blood and brain microdialysate samples: application to pharmacokinetic/pharmacodynamic studies in rats. *J.Chromatogr.B Analyt.Technol.Biomed.Life Sci.* **822**: 230-237
- Groenendaal D, Freijer J, de Mik D, Bouw MR, Danhof M, Lange EC (2007) Influence of biophase distribution and P-glycoprotein interaction on pharmacokinetic-pharmacodynamic modelling of the effects of morphine on the EEG. *Br.J.Pharmacol.* **515**: 713-720
- Henthorn TK, Liu Y, Mahapatro M, Ng KY (1999) Active transport of fentanyl by the blood-brain barrier. *J.Pharmacol. Exp. Ther.* **289**: 1084-1089
- Letrent SP, Pollack GM, Brouwer KR, Brouwer KL (1998) Effect of GF120918, a potent P-glycoprotein inhibitor, on morphine pharmacokinetics and pharmacodynamics in the rat. *Pharm.Res.* **15**: 599-605

## ROLE OF COMPLEX BIOPHASE DISTRIBUTION KINETICS

---

Letrement SP, Pollack GM, Brouwer KR, Brouwer KL (1999a) Effects of a potent and specific P-glycoprotein inhibitor on the blood- brain barrier distribution and antinociceptive effect of morphine in the rat. *Drug Metab Dispos.* **27**: 827-834

Letrement SP, Polli JW, Humphreys JE, Pollack GM, Brouwer KR, Brouwer KL (1999b) P-glycoprotein-mediated transport of morphine in brain capillary endothelial cells. *Biochem.Pharmacol.* **58**: 951-957

Liu X, Smith BJ, Chen C, Callegari E, Becker SL, Chen X, Cianfrogna J, Doran AC, Doran SD, Gibbs JP, Hosea N, Liu J, Nelson FR, Szewc MA, Van Deusen J (2005) Use of a physiologically based pharmacokinetic model to study the time to reach brain equilibrium: an experimental analysis of the role of blood-brain barrier permeability, plasma protein binding, and brain tissue binding. *J.Pharmacol.Exp.Ther.* **313**: 1254-1262

Mahar Doan KM, Humphreys JE, Webster LO, Wring SA, Shampine LJ, Serabjit-Singh CJ, Adkison KK, Polli JW (2002) Passive permeability and P-glycoprotein-mediated efflux differentiate central nervous system (CNS) and non-CNS marketed drugs. *J.Pharmacol.Exp.Ther.* **303**: 1029-1037

Mandema JW, Danhof M (1990) Pharmacokinetic-pharmacodynamic modeling of the central nervous system effects of heptabarbital using aperiodic EEG analysis. *J.Pharmacokinetic.Biopharm.* **18**: 459-481

Mandema JW, Tukker E, Danhof M (1991a) Pharmacokinetic-pharmacodynamic modelling of the EEG effects of midazolam in individual rats: influence of rate and route of administration. *Br.J.Pharmacol* **102**: 663-668

Mandema JW, Veng-Pedersen P, Danhof M (1991b) Estimation of amobarbital plasma-effect site equilibration kinetics. Relevance of polyexponential conductance functions. *J.Pharmacokinetic.Biopharm.* **19**: 617-634

Platts JA, Butina D, Abraham MH, Hersey A (1999) Estimation of molecular linear free energy relation descriptors using a group contribution approach. *J.Chem.Inform.Comp.Sci.* **39**: 835-845

Schinkel AH, Wagenaar E, Mol CA, van Deemter L (1996) P-glycoprotein in the blood-brain barrier of mice influences the brain penetration and pharmacological activity of many drugs. *J.Clin.Invest* **97**: 2517-2524

Schinkel AH, Wagenaar E, van Deemter L, Mol CA, Borst P (1995) Absence of the mdr1a P-Glycoprotein in mice affects tissue distribution and pharmacokinetics of dexamethasone, digoxin, and cyclosporin A. *J.Clin.Invest* **96**: 1698-1705

Sheiner LB, Stanski DR, Vozeh S, Miller RD, Ham J (1979) Simultaneous modeling of pharmacokinetics and pharmacodynamics: application to d-tubocurarine. *Clin Pharmacol Ther* **25**: 358-371

Tran TT, Mittal A, Aldinger T, Polli JW, Ayrton A, Ellens H, Bentz J (2005) The elementary mass action rate constants of P-gp transport for a confluent monolayer of MDCKII-hMDR1 cells. *Biophysical Journal* **88**: 715-738

Tran TT, Mittal A, Gales T, Maleeff B, Aldinger T, Polli JW, Ayrton A, Ellens H, Bentz J (2004) Exact kinetic analysis of passive transport across a polarized confluent MDCK cell monolayer modeled as a single barrier. *J. Pharm.Sci.* **93**: 2108-2123

Visser SA, Smulders CJ, Reijers BP, van der Graaf PH, Peletier LA, Danhof M (2002) Mechanism-based pharmacokinetic-pharmacodynamic modeling of concentration-dependent hysteresis and biphasic electroencephalogram effects of alphaxalone in rats. *J.Pharmacol Exp.Ther* **302**: 1158-1167

Wagner JG (1974) A safe method for rapidly achieving plasma concentration plateaus. *Clin.Pharmacol.Ther.* **16**: 691-700

Wandel C, Kim R, Wood M, Wood A (2002) Interaction of morphine, fentanyl, sufentanil, alfentanil, and loperamide with the efflux drug transporter P-glycoprotein. *Anesthesiology* **96**: 913-920

Yano Y, Beal SL, Sheiner LB (2001) Evaluating pharmacokinetic/pharmacodynamic models using the posterior predictive check. *J.Pharmacokinet.Pharmacodyn.* **28**: 171-192





